Cisplatin-resistant germ cell tumor models: An exploration of the epithelial-mesenchymal transition regulator *SLUG*

INGRIDY IZABELLA VIEIRA CARDOSO[1], MARCELA NUNES ROSA[1], DANIEL ANTUNES MORENO[1], LETÍCIA MARIA BARBOSA TUFI[1], LORRAYNE PEREIRA RAMOS[1], LARISSA ALESSANDRA BOURDETH PEREIRA[1], LENILSON SILVA[1], JANAINA MELLO SOARES GALVÃO[1], ISABELA CRISTIANE TOSI[1], ANDRÉ VAN HELVOORT LENGERT[1], MARCELO CAVALCANTI DA CRUZ[2], SILVIA APARECIDA TEIXEIRA[1], RUI MANUEL REIS[1,3], LUIZ FERNANDO LOPES[4] and MARIANA TOMAZINI PINTO[1,4]

[1]Molecular Oncology Research Center, Barretos Cancer Hospital, Barretos, São Paulo 14784400, Brazil; [2]Department of Pathology, Barretos Cancer Hospital, Barretos, São Paulo 14784400, Brazil; [3]Life and Health Sciences Research Institute Medical School, University of Minho, 4710057 Braga, Portugal; [4]Barretos Children's Cancer Hospital, Hospital de Amor, Barretos, São Paulo 14784400, Brazil

Received February 28, 2024; Accepted July 2, 2024

DOI: 10.3892/mmr.2024.13352

Abstract. Germ cell tumors (GCTs) constitute diverse neoplasms arising in the gonads or extragonadal locations. Testicular GCTs (TGCTs) are the predominant solid tumors in adolescents and young men. Despite cisplatin serving as the primary therapeutic intervention for TGCTs, 10-20% of patients with advanced disease demonstrate resistance to cisplatin-based chemotherapy, and epithelial-mesenchymal transition (EMT) is a potential contributor to this resistance. EMT is regulated by various factors, including the snail family transcriptional repressor 2 (*SLUG)* transcriptional factor, and, to the best of our knowledge, remains unexplored within TGCTs. Therefore, the present study investigated the EMT transcription factor *SLUG* in TGCTs. *In silico* analyses were performed to investigate the expression of EMT markers in TGCTs. In addition, a cisplatin-resistant model for TGCTs was developed using the NTERA-2 cell line, and a mouse model was also established. Subsequently, EMT was assessed both *in vitro* and *in vivo* within the cisplatin-resistant models using quantitative PCR and western blot analyses. The results of the *in silico* analysis showed that the different histologies exhibited distinct expression profiles for EMT markers. Seminomas exhibited a lower expression of EMT markers, whereas embryonal carcinomas and mixed GCT demonstrated high expression. Notably, patients with lower *SLUG* expression had longer median progression-free survival (46.4 months vs. 28.0 months, P=0.022). In the *in vitro* analysis, EMT-associated genes [fibronectin; vimentin (*VIM*); actin, α2, smooth muscle; collagen type I α1; transforming growth factor-β1; and *SLUG*] were upregulated in the cisplatin-resistant NTERA-2 (NTERA-2R) cell line after 72 h of cisplatin treatment. Consistent with this finding, the NTERA-2R mouse model demonstrated a significant upregulation in the expression levels of *VIM* and *SLUG*. In conclusion, the present findings suggested that *SLUG* may serve a crucial role in connecting EMT with the development of cisplatin resistance, and targeting *SLUG* may be a putative therapeutic strategy to mitigate cisplatin resistance.

Correspondence to: Dr Mariana Tomazini Pinto, Molecular Oncology Research Center, Barretos Cancer Hospital, 1332 Antenor Duarte Villela Street, Barretos, São Paulo 14784400, Brazil
E-mail: mariana.pinto49@edu.hospitaldeamor.com.br

Key words: epithelial-mesenchymal transition, SLUG, germ cell tumor, cisplatin resistance

Introduction

Epithelial-mesenchymal transition (EMT) results in the loss of epithelial features and the gain of a mesenchymal phenotype in cells; this is essential during embryonic development and in some diseases, such as cancer (1,2). EMT is executed by EMT-activating transcription factors (EMT-TFs), mainly snail family transcriptional repressor 1 (*SNAIL*) and snail family transcriptional repressor 2 (*SLUG*). Over the last decade, these EMT-TFs have demonstrated crucial roles in all stages of cancer progression, including primary tumor growth, invasion, dissemination, metastasis, cancer stem cell properties and resistance to therapy (3-5). Several studies have described the roles of EMT programs in various types of cancer (6-8); however, more information is needed regarding germ cell tumors (GCTs).

GCTs comprise a heterogeneous group of neoplasms occurring in the gonads (ovaries or testes) or at extragonadal locations (9). Testicular GCTs (TGCTs) are the most common solid tumors in adolescents and young men (10), and are

organized into two histological groups: Seminoma (SE) and non-seminoma GCTs (NSGCTs). NSGCTs are subdivided into the following categories: Embryonal carcinoma, yolk sac tumor, teratoma, choriocarcinoma and mixed NSGCT, in which more than one histological type occurs (11). Cisplatin is the most commonly used drug in the treatment of TGCTs (12,13); however, 10-20% of patients with advanced disease demonstrate resistance to cisplatin-based chemotherapy (14). The resistance of TGCT to cisplatin chemotherapy may be related to different molecular mechanisms, including EMT. Evidence has suggested that the EMT process may serve an important role in the development of chemoresistance by altering the expression of essential genes involved in cell cycle regulation, drug transport and apoptosis (15-17).

SLUG expression has emerged as a valuable prognostic indicator for various types of cancer. In gastric cancer, its utility extends to predicting lymph node metastasis and influencing overall patient survival (18). SLUG also has been implicated in tumor metastasis and angiogenesis in ovarian cancer (19). Furthermore, elevated SLUG expression in non-small cell lung cancer has been significantly linked to an increased rate of cancer recurrence and diminished overall survival (20). Despite these extensive associations in various malignancies, there remains a paucity of studies exploring EMT in TGCT. Therefore, the present study aimed to investigate the EMT transcription factor *SLUG* in TGCTs.

Materials and methods

In silico data analyses. Patient clinical and pathological information, along with gene expression data, were obtained from the Testicular Germ Cell Tumors RNA sequencing dataset from The Cancer Genome Atlas (TCGA Pan-Cancer Atlas; TCGA-TGCT dataset) (21) available on the cBioPortal (https://www.cbioportal.org/). The present study focused on patients diagnosed with SE, embryonal carcinoma and mixed NSGCTs.

The expression of EMT-related genes in these histological types was examined to explore their potential role in TGCT. Using the z-score transformed data of the EMT-related genes, a heatmap was generated to visually analyze the gene expression patterns, created with the ComplexHeatmap package version 2.16.0 (22). Patients with available information on progression-free survival (PFS) in 5 years, as well as gene expression data for *SNAI1* (also referred to as *SNAIL*) and *SNAI2* (also referred to as *SLUG*) obtained from RNA sequencing assays (Illumina HiSeq_RNASeqV2), were selected. The present analysis included 89 TGCT cases with both survival and mRNA expression information. Patients were classified into low and high expression groups according to the median value of *SNAIL* and *SLUG* expression.

Cell culture. Human NTERA-2 clone D1 [NT2/D1] and JEG-3 cells were used in the present study. NTERA-2 clone D1 (cat. no. 01071221, RRID: CVCL_3407; European Collection of Authenticated Cell Cultures) is a cell line derived from a human testicular embryonal carcinoma, and the JEG-3 cell line is derived from a human placenta choriocarcinoma (cat. no. HTB-36, RRID: CVCL_0363; American Type Culture Collection). Cells were cultured according to the supplier's instructions in Dulbecco's modified Eagle's medium (Thermo Fisher Scientific, Inc.) supplemented with 10% heat-inactivated fetal bovine serum (Corning, Inc.), 100 U/ml penicillin and 100 mg/ml streptomycin (Corning, Inc.) at 37˚C in 5% CO_2. Our group previously published a study in which a cisplatin-resistant cell model was developed by growing the NTERA-2 clone D1 cell line in increasing concentrations of cisplatin over a period of ~8 months (23). This model was utilized in the current study and the parental NTERA-2 (NTERA-2P) and cisplatin-resistant NTERA-2 (NTERA-2R) cell lines were cultured in the same conditions. Cisplatin (cat. no. PHR1624; Sigma-Aldrich; Merck KGaA) was prepared at 5 mM in 0.9% NaCl. NTERA-2 cells were treated with the IC_{50} dose of cisplatin and were collected after 72 h for gene expression analysis. All cell lines were mycoplasma-free (MycoAlert Mycoplasma Detection Kit; Lonza Group Ltd.; tested monthly) and were authenticated by short tandem-repeat analysis at the Barretos Cancer Hospital facilities (Barretos, Brazil) (24). For gene expression characterization of JEG-3 and NTERA-2P cells, cells were not treated. For gene expression comparisons between NTERA-2P and NTERA-2R cells, cells were treated with the IC_{50} of cisplatin (0.25 μM for NTERA-2P cells and 5 μM for NTERA-2R cells) and were collected after 72 h.

RNA isolation and reverse transcription-quantitative PCR. Total RNA was extracted from cells or frozen mouse tumor tissues using TRIzol® Reagent (Invitrogen; Thermo Fisher Scientific, Inc.), and RT was performed using the High-Capacity cDNA Reverse Transcription kit (Thermo Fisher Scientific, Inc.), according to the manufacturer's protocol. Gene expression analysis was performed by qPCR (thermocycling conditions: 50˚C for 2 min and 95˚C for 10 min, followed by 40 cycles of 95˚C for 15 sec and 60˚C for 1 min) using TaqMan® Gene Expression Assays (Thermo Fisher Scientific, Inc.) and a QuantStudio 6 real-time system (Thermo Fisher Scientific, Inc.) for the following genes: Cadherin 1 (*CDH1*; assay ID Hs00170423_m1), cadherin 2 (*CDH2*; assay ID Hs00983056_m1), fibronectin (*FN1*; assay ID Hs01549976_m1), vimentin (*VIM*; assay ID Hs00185584_m1), actin, α2, smooth muscle (*ACTA2*; assay ID Hs00909449_m1), collagen type I α1 (*COL1A1*; assay ID Hs00164004 m1), transforming growth factor-β1 (*TGF-β*; assay ID Hs00998133_m1), *SNAIL* (assay ID Hs00195591_m1) and *SLUG* (assay ID Hs00950344_m1). Glyceraldehyde-3-phosphate dehydrogenase (cat. no. 4310884E) was used to normalize the mRNA amount for each sample. The relative expression unit (REU) method ($REU=10.000/2^{\Delta Ct}$) was used to calculate the REUs, and the $2^{-\Delta\Delta Cq}$ method was used to calculate the relative gene expression levels (25).

Western blot analysis. Total proteins were extracted from cells using RIPA buffer (Sigma-Aldrich; Merck KGaA), including 10% protease and phosphatase inhibitors (Sigma-Aldrich; Merck KGaA). After 15 min on ice, samples were centrifuged at 13,000 x g for 30 min at 4˚C, the supernatant was collected, and protein concentration was quantified using the Bradford assay (Bio-Rad Laboratories, Inc.). Proteins (50 μg) were then denatured at 95˚C for 5 min in 4X Laemmli buffer (Thermo Fisher Scientific, Inc.), separated by SDS-PAGE on

10% polyacrylamide gels and transferred onto nitrocellulose membranes (Amersham Protran; Cytiva). Membranes were blocked in 5% milk powder in TBS/0.1% Tween (pH 7.6) for 1 h at room temperature and were then incubated with the following primary antibodies overnight at 4˚C: CDH1 (1:500; cat. no. 3195S), CDH2 (1:500; cat. no. 4061S), and VIM (1:1,000; cat. no. 5741S), all from Cell Signaling Technology, Inc. β-actin was used as a loading control (1:1,000; cat. no. 8457; Cell Signaling Technology, Inc.). Subsequently, the membranes were incubated with horseradish peroxidase-conjugated secondary antibodies (1:5,000; cat. no. 7074P2; Cell Signaling Technology, Inc.) for 1 h at room temperature. The blots were detected by chemiluminescence using either SignalFire ECL Reagent (Cell Signaling Technology, Inc.) or SuperSignal West Femto Maximum Sensitivity Substrate (Thermo Fisher Scientific, Inc.). The chemiluminescent signal was detected using ImageQuant LAS 4000 mini (Cytiva), and densitometric analysis was performed using ImageJ software, version 1.4 (National Institutes of Health).

Animals. Athymic nude mice (Mus musculus) were purchased from Jackson Laboratory and were housed in microisolator cages under specific pathogen-free conditions at a temperature of 21˚C and a humidity of 55% at the Animal Facility, Barretos Cancer Hospital (26). Mice received ad libitum access to sterile food and water, and were maintained under a 12-h light/dark cycle. All animal experiments were performed according to protocols approved by the Institutional Animal Care and Use Committee (IACUC) following Brazil's National Council for Animal Experimentation Control guidelines (law no. 11,794 of October 8, 2008; decree 6,899 of June 15, 2009). All animal experiments were approved by the IACUC at Barretos Cancer Hospital (approval no. 010/2020).

For experiments, $1x10^6$ NTERA-2P or NTERA-2R cells were resuspended in 100 μl HBSS (HyClone; Cytiva)/Matrigel (Corning, Inc.) (1:1 volume). The cells were subcutaneously engrafted into the right flank of 6-8-week-old male mice (n=3 mice/group; weight, ~28 g). The total number of animals was 6 (3 animals per group; two groups). The animals were monitored for signs of morbidity, and symptoms such as weight loss exceeding 20% and difficulty walking or eating were used as criteria to halt the experiments and sacrifice the mice. Notably, in the present study, it was not necessary to interrupt the experiments for any reason. The weights of the mice were recorded twice weekly and tumor volume (V) was measured with a caliper and calculated using the formula: $V=(Dxd)^2x0.5$ where D represents the longest diameter and d the smallest diameter of the tumor. The endpoint for euthanizing the animals was when the tumor volume reached ~2,000 mm^3. The mice were euthanized using an intraperitoneal injection of a combination of ketamine (300 mg/kg) and xylazine (30 mg/kg). Subsequently, tumors were aseptically excised, and a portion was subjected to formalin fixation for histological analysis, whereas another portion was rapidly frozen in liquid nitrogen and stored at -80˚C for RNA extraction.

The frozen tumor was macerated using a pestle and mortar, and the resulting material was subsequently transferred to a microtube where, 1.5 ml TRIzol was added. After homogenization, RNA extraction proceeded according to the manufacturer's instructions, and RNA quantification was conducted using a Nanodrop instrument (Thermo Fisher Scientific, Inc.). RT-qPCR was performed as aforementioned.

For histological analysis, tissues were harvested and fixed in 4% paraformaldehyde at 25˚C for 24 h. Sections were then dehydrated, embedded in paraffin and cut into 4-μm slices using a microtome. These sections were stained at room temperature with hematoxylin (ready-to-use; cat. no. CS70030-2; Dako; Agilent Technologies, Inc.) and eosin (ready-to-use; cat. No CS 70130-2; Dako; Agilent Technologies, Inc.) using an automated platform and subsequently reviewed by a pathologist under a light microscope. To assess cell proliferation in NTERA-2P and NTERA-2R tumors, immunohistochemical staining of Ki-67 (ready-to-use; cat. no. IR626; Dako; Agilent Technologies, Inc.) was conducted. Briefly, the tissue sections were deparaffinized (75˚C for 4 min) and subjected to antigen retrieval in conditioning solution at 95˚C for 64 min. Primary antibody (ki-67) was added, and detection was performed using the Ultra View Universal DAB Detection kit (cat. no. 760-500; Roche Diagnostics). These procedures (H&E and ki-67 staining) were conducted using the Ventana BenchMark Ultra® automated platform (Roche Tissue Diagnostics) at the Department of Pathology, Barretos Cancer Hospital. The experiments were performed using the automated platform and details such as the dilution and percentage of the antibodies and reagents were not provided by the manufacturers. Slides were scanned using an Aperio CS2 scanner (Leica Microsystems, Inc.).

Statistical analysis. All data are presented as the mean ± standard deviation. Unpaired Student's t-test and non-parametric Mann-Whitney two-tailed test were used to compare two groups. One-way ANOVA was used to compare multiple treatment groups, followed by Tukey's multiple comparisons test. All statistical tests were performed using GraphPad Prism (version 8.0.2; Dotmatics) software. IBM SPSS Statistics version 25 software (IBM Corp.) was used for survival analysis, which was performed using the Kaplan-Meier method and log-rank test. For multiple comparisons, Bonferroni correction was applied following log-rank test. $P \leq 0.05$ was considered to indicate a statistically significant difference.

Results

In silico analysis. To evaluate EMT-associated genes, the online tool cBioPortal was used. The dataset from the Testicular Germ Cell Cancer study previously reported by Shen *et al* (21) was analyzed, which included 89 patients with TGCT, including 49 SEs, 29 mixed tumors and 11 embryonal carcinomas. The expression levels of EMT-associated genes were evaluated (Fig. 1) and the patients were shown to be divided into two main groups according to their histology: i) Embryonal carcinoma and mixed GCT, and ii) SE (Fig. 1A). Three patients with mixed GCT were classified in the SE group, which can be explained by the presence of an SE component (TCGA-2G-AAH3-01: 60% teratoma mature and immature, 35% SE, yolk sac tumor 5%; TCGA-2G-AAH0-01: 95% SE and 5% yolk sac tumor; TCGA-SN-A6IS-01: 85% SE and 15% teratoma mature). For TCGA-2G-AAH3-01, despite teratoma being the predominant component, it was classified in the SE group due to the significant presence of seminoma (35%), as teratomas were not classified separately. The distinct

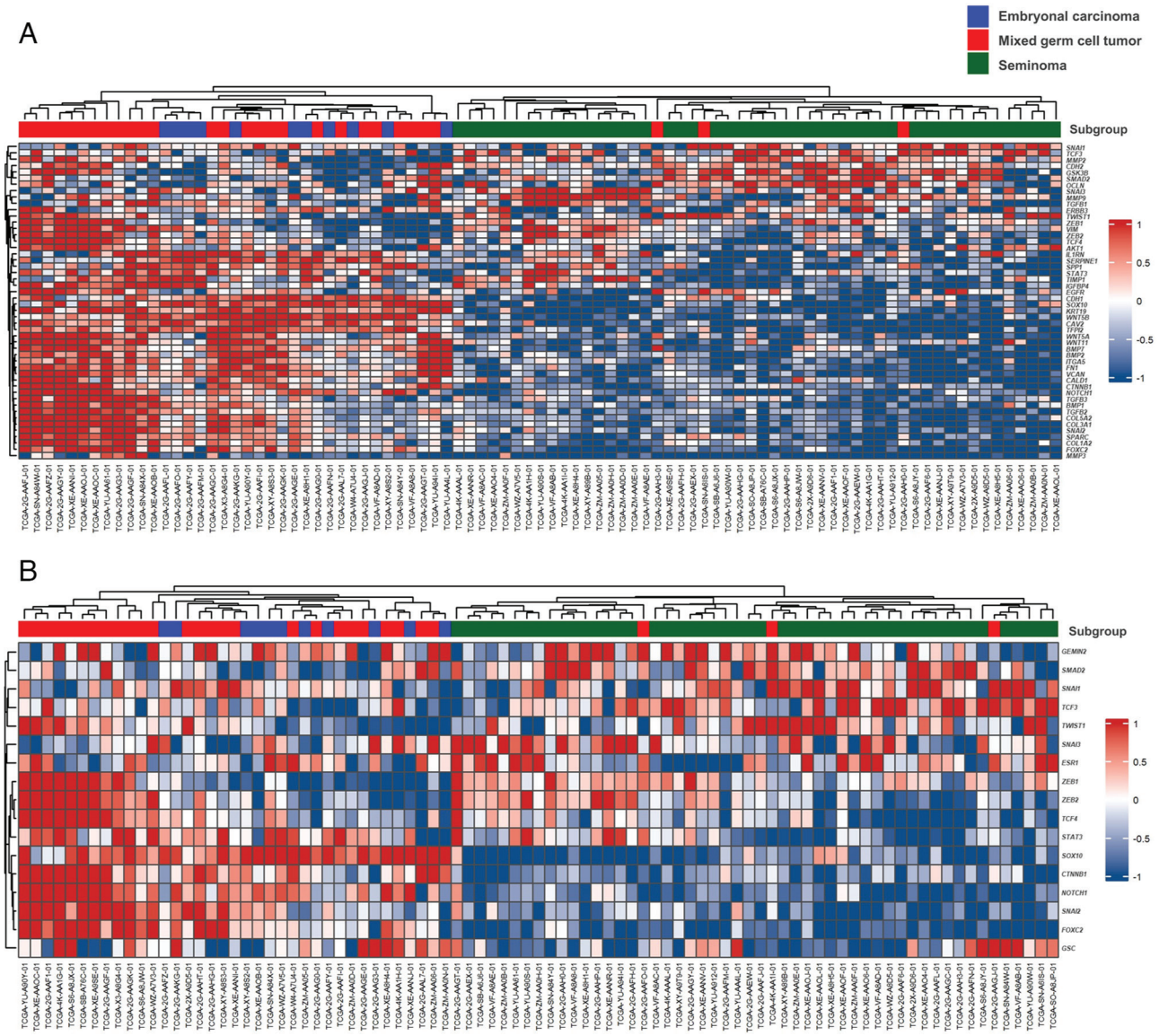

Figure 1. Heatmap and dendrogram of EMT-related genes. The expression levels were used to group the gene profiles according to their similarities, and the gene expression profiles of each histology were compared to each other. (A) Heatmap of the most significant genes associated with EMT. (B) Heatmap of EMT-related transcription factors. Rows indicate the relative expression levels for a single gene, and columns indicate the expression level for a single sample. Blue and red indicate the genes with lower and higher expression levels, respectively. EMT, epithelial-mesenchymal transition; TCGA, The Cancer Genome Atlas.

histologies exhibited disparate expression profiles for EMT markers. The SE group exhibited lower expression of EMT markers, whereas the embryonal carcinoma and mixed GCT group showed high expression of EMT markers, suggesting that the profile of EMT markers varies according to histology. A second analysis was performed, considering only EMT-TFs (Fig. 1B). Embryonal carcinoma and mixed GCT exhibited high expression levels of some transcription factors, such as *SLUG*, *SOX10* and *NOTCH1*, whereas SE had high expression levels of *SNAIL* and *TCF3*. These results suggested that the expression of EMT-associated genes may be associated with clinicopathological features, indicating that EMT markers may be relevant for classifying the histology of GCTs.

According to the analyses, *SNAIL* and *SLUG* exhibited different expression levels in each histology. To clarify the expression of *SNAIL* and *SLUG* in TGCTs, the expression of these factors was evaluated individually in the three histological types (embryonal carcinoma, mixed GCT and SE). The results showed a significant difference in the expression of *SLUG* (Fig. 2A). *SLUG* was significantly upregulated in Mixed GCT compared with embryonal carcinoma and SE. No significant difference was observed in *SNAIL* expression (Fig. 2B).

The PFS of all patients was assessed, and patients with SE histology had a higher PFS compared with those with embryonal carcinoma (49.9 months vs. 27.6 months) and mixed GCT (49.9 months vs. 28.6 months) (Fig. 3A).

When analyzing individual the transcription factors *SNAIL* and *SLUG*, although not statistically significant, patients with lower and higher *SNAIL* expression had median PFS durations of 47.2 and 29.7 months, respectively (Fig. 3B). In addition, patients with lower *SLUG* expression had a median PFS of 46.4 months, compared to 28.0 months for those with higher *SLUG* expression (Fig. 3C). These findings highlight the

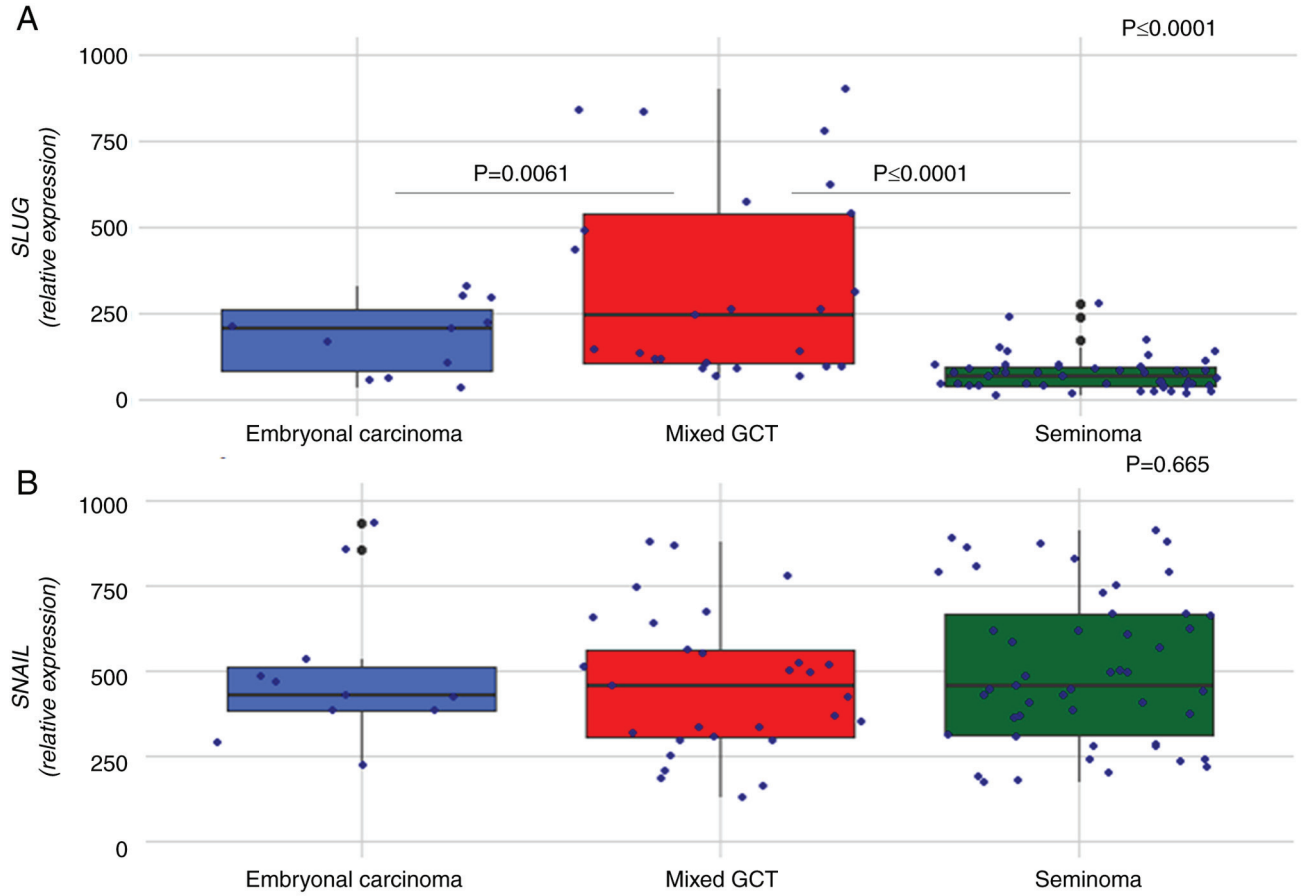

Figure 2. Boxplot of *SNAIL* and *SLUG* expression in testicular GCT. Expression of (A) *SLUG* and (B) *SNAIL* in embryonal carcinoma, mixed GCT and seminoma. GCT, germ cell tumor; *SLUG*, snail family transcriptional repressor 2; *SNAIL*, snail family transcriptional repressor 1.

significant effects of *SLUG* expression on PFS in patients with TGCT, suggesting that this EMT transcriptional regulator may be a potential prognostic marker and therapeutic target for GCTs (27).

Subsequently, an integrated analysis was performed to examine the differences in PFS of patients with both high and low levels of *SNAIL* and *SLUG*. The Snail superfamily of transcription factors encompasses SNAIL, SLUG and SCRATCH proteins, characterized by their possession of a SNAG domain and a minimum of four functional zinc fingers. Through comparative analysis of these zinc-finger sequences, the superfamily has been delineated into SNAIL and SCRATCH families, with SLUG designated as a subfamily within the SNAIL group (5). Based on this evidence, integrated analyses were performed to verify the distinct impact of *SNAIL* and *SLUG*. Patients expressing low levels of both factors ($SNAIL^{low}SLUG^{low}$) had a higher PFS compared to those with high expression of both transcription factors ($SNAIL^{high}SLUG^{high}$); the respective median PFS durations were 54.3 and 16.5 months (Fig. 3D). In addition, patients in the $SNAIL^{low}SLUG^{low}$ group had a higher PFS compared to those with high *SNAIL* expression and low *SLUG* expression ($SNAIL^{high}SLUG^{low}$), with median PFS durations of 54.3 and 34.1 months (Fig. 3D). Although the difference in PFS between $SNAIL^{low}SLUG^{low}$ and $SNAIL^{low}SLUG^{high}$ groups did not reach statistical significance, there was a trend favoring higher PFS in the $SNAIL^{low}SLUG^{high}$ group (54.3 months vs. 31.1 months; Fig. 3D). In addition, the association between the expression levels of the transcription factors *SNAIL* and *SLUG*, both individually and combined, with PFS was analyzed in the distinct GCT histologies: Mixed tumor, SE and embryonal carcinoma.

The Bonferroni correction was performed after each log-rank test to account for multiple comparisons. However, for the SE ($SNAIL^{low}SLUG^{low}$) and embryonal carcinoma ($SNAIL^{low}SLUG^{high}$) groups, all samples were censored; therefore, it was not possible to calculate the averages for these groups. *SNAIL* and *SLUG* expression had no significant effect on PFS across the various histological types of GCTs, including SE, mixed GCT and embryonal carcinoma (Fig. S1). However, a trend emerged when all tumor types were analyzed collectively (Fig. 3), revealing an association between PFS and *SLUG* expression. This apparent discrepancy may be justified by the low number of samples within each histological subgroup, which could result in a loss of statistical power, thereby obscuring potential associations that become apparent only when the sample size is increased by combining all tumor types.

Expression of EMT markers in GCT cell lines. Since EMT markers were associated with the histological classification of GCTs, and due to their effects on PFS, the mRNA expression levels of some EMT markers were examined in GCT cell lines (Fig. 4A). Compared with in JEG-3 cells, the NTERA-2 cell

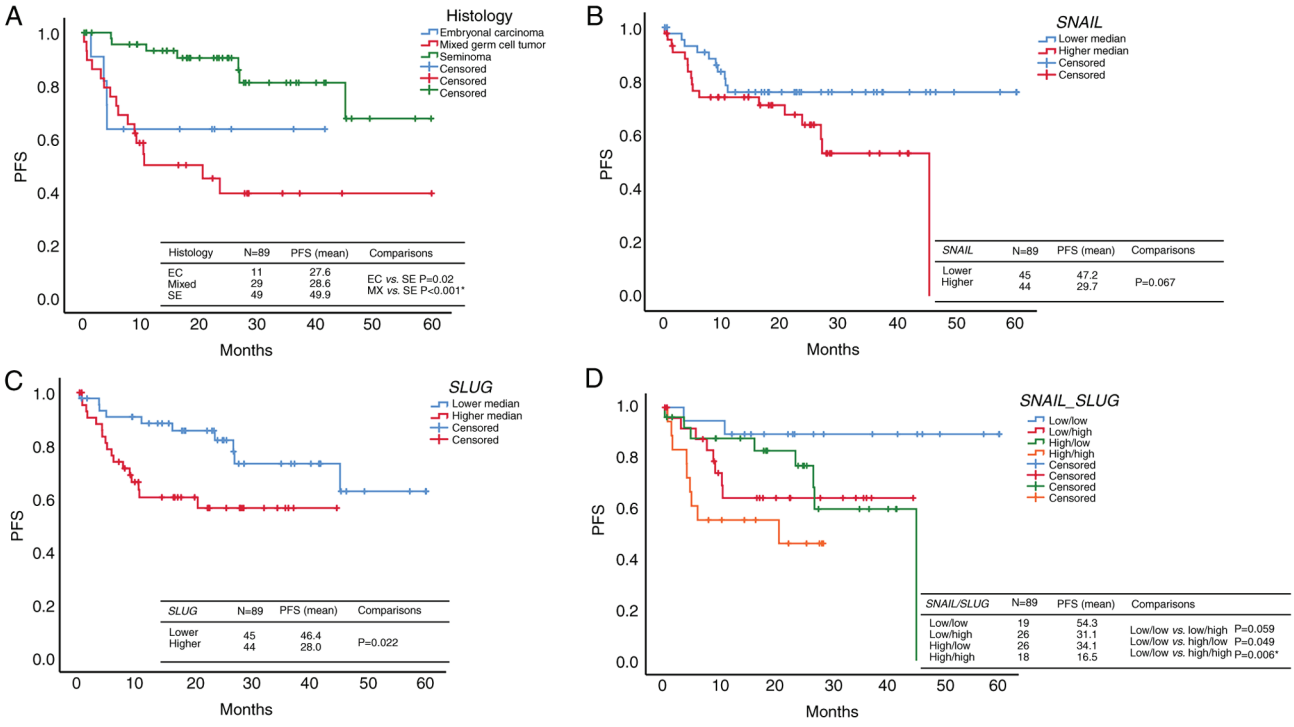

Figure 3. PFS of patients with testicular germ cell tumor. (A) Association of SE, MX and EC histological types with PFS. Association of the individual expression of (B) *SNAIL* and (C) *SLUG* transcription factors with PFS. (D) Association of the combination of *SNAIL* and *SLUG* expression with PFS. Bonferroni correction was applied after the log-rank test with $\alpha=0.05/3=0.0167$ for (A), and $\alpha=0.05/6=0.0083$ for (D). *Significant value for log-rank + Bonferroni. P-values equal to or less than the Bonferroni correction threshold were considered significant. EC, embryonal carcinoma; MX, mixed germ cell tumor; PFS, progression-free survival; SE, seminoma; *SLUG*, snail family transcriptional repressor 2; *SNAIL*, snail family transcriptional repressor 1.

line exhibited increased expression levels of mesenchymal markers, such as *CDH2*, *VIM* and *SLUG*, and decreased *CDH1* and *SNAIL* expression. This difference in the expression of EMT-associated markers in both cell lines may be attributed to the distinct histological characteristics of the NTERA-2 (embryonal carcinoma) and JEG-3 (choriocarcinoma) lineages. Therefore, these data indicates a potential association between EMT-associated genes and clinical parameters in GCTs, particularly with regard to the embryonal carcinoma histological subtype.

It has been reported that ~15% of patients with GCT are resistant to cisplatin-based chemotherapy (14,28), and the EMT process may serve a role in developing chemoresistance (29,30). Our previous study created an *in vitro* TGCT cisplatin-resistant model using the NTERA-2 cell line (23). Using this model, the present study investigated the expression levels of EMT-associated genes, and revealed that *FN1*, *VIM*, *ACTA2*, *COL1A1*, *TGF-β* and *SLUG* were significantly upregulated in NTERA-2R cells compared with those in the NTERA-2P cell line, and *CDH1* expression exhibited an increasing trend (Fig. 4B), after 72 h of cisplatin treatment. In addition, *CDH2* expression exhibited a decreasing trend in NTERA-2R cells, whereas there was no notable difference in *SNAIL* expression levels. Consistent with these findings, there was a trend toward higher levels of CDH1 protein, whereas the protein expression levels of CDH2 tended to decrease in NTERA-2R cells (Fig. S2). By contrast, there was no difference in VIM protein expression between the cell lines. Overall, these data suggested that EMT may be a critical factor in chemoresistance.

Expression of EMT-associated genes in a cisplatin-resistant mouse model of GCT. To validate whether EMT is a key factor in chemoresistance, NTERA-2P and NTERA-2R cells were implanted subcutaneously into nude mice (Fig. 5A). H&E staining and the expression levels of Ki-67, which is used as a proliferative marker (31,32), were comparable between the NTERA-2P and NTERA-2R groups. The tumors from both the NTERA-2P and NTERA-2R groups took 15-34 days to start growing after cell inoculation, when the nodule was visible enough to be measurable (Fig. 5B). Both NTERA-2P and NTERA-2R cells grew gradually in the animals. In the NTERA-2P group, the tumors took 30 to 53 days from the beginning until they reached ~2,000 mm^3 in volume. In the NTERA-2R group the tumors took 25 to 37 days for this growth, which was similar to the NTERA-2P group.

Consistent with the findings observed *in vitro*, the NTERA-2R mouse model demonstrated a significant upregulation in the expression of *VIM* and *SLUG* (Fig. 5C), suggesting that *SLUG* may serve as the pivotal transcription factor bridging the association between EMT and cisplatin resistance.

Discussion

Between 10 and 20% of patients with TGCT have been reported to be resistant to cisplatin-based chemotherapy (14,33) and several molecular mechanisms have been shown to be related to chemoresistance, including the EMT process (34,35). The present study evaluated the role of the EMT-TF *SLUG* in TGCT. Overall, EMT markers were associated with

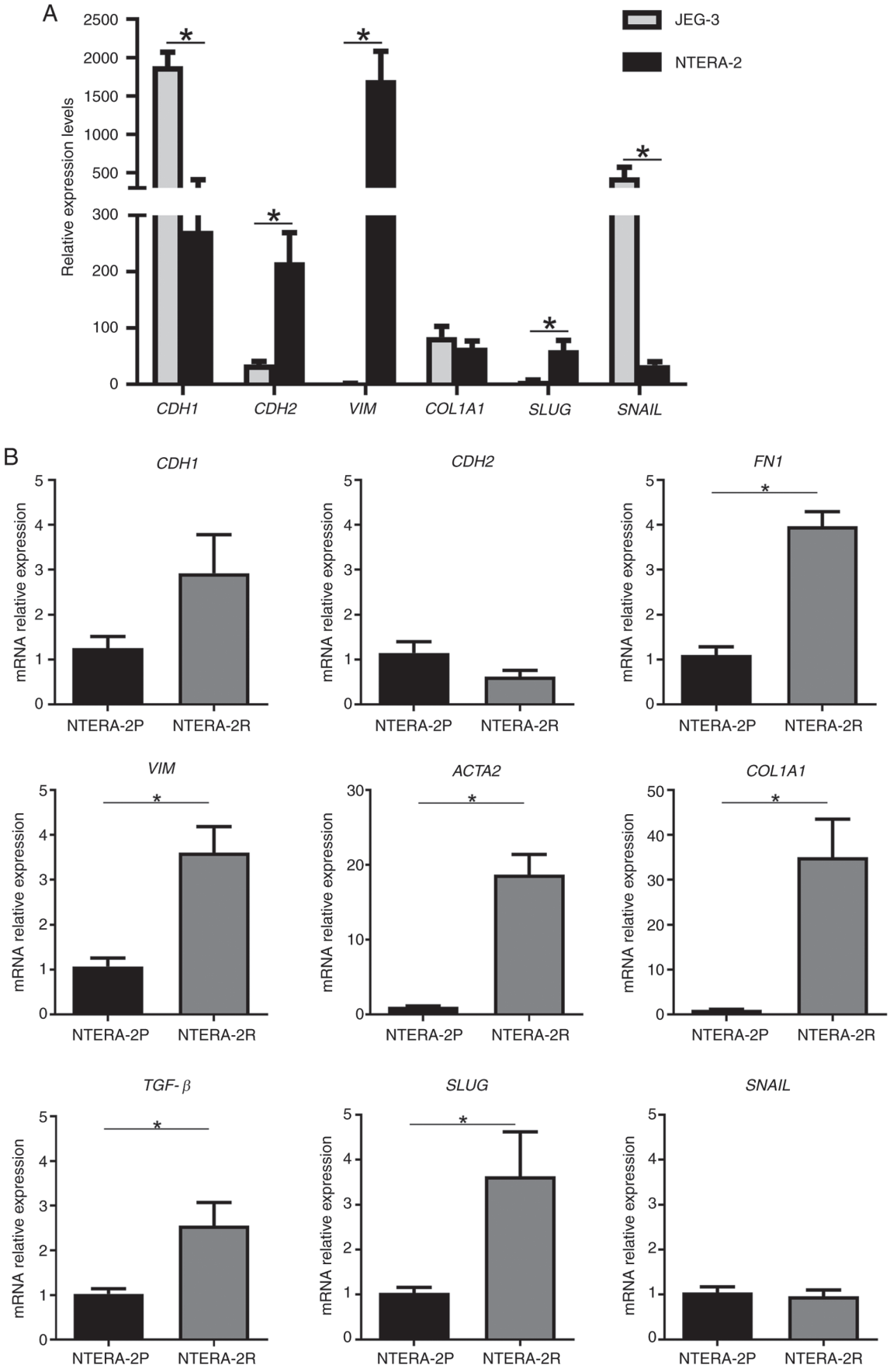

Figure 4. Expression of epithelial-mesenchymal transition-associated genes in germ cell tumor cell lines. (A) Relative expression levels of *CDH1*, *CDH2*, *VIM*, *COL1A1*, *SLUG* and *SNAIL* in NTERA-2 and JEG-3 cell lines. (B) Relative mRNA expression levels of *CDH1*, *CDH2*, *FN1*, *VIM*, *ACTA2*, *COL1A1*, *TGF-β*, *SLUG* and *SNAIL* in NTERA-2P and NTERA-2R cells after 72 h of cisplatin treatment. *P≤0.05. *ACTA2*, actin, α2, smooth muscle; *COL1A1*, collagen type I α1; *CDH*, cadherin; *FN1*, fibronectin; NTERA-2P, parental NTERA-2; NTERA-2R, cisplatin-resistant NTERA-2; *SLUG*, snail family transcriptional repressor 2; SNAIL, snail family transcriptional repressor 1; *TGF-β*, transforming growth factor-β1; *VIM*, vimentin.

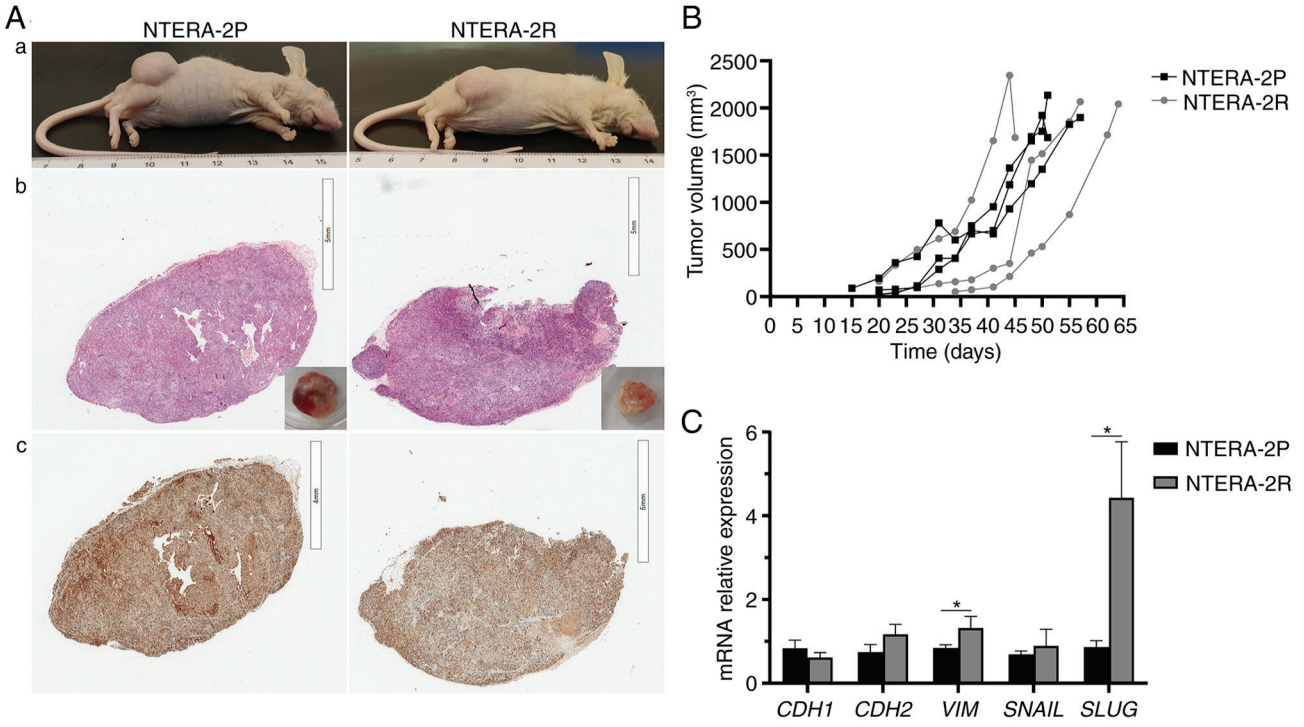

Figure 5. Animal models of germ cell tumors. (A) Representative images of a xenograft model of NTERA-2P and NTERA-2R. (Aa) Images of solid tumors. (Ab) Hematoxylin and eosin staining of NTERA-2P and NTERA-2R tumors (scale bars, 5 mm). (Ac) Expression of Ki-67 in NTERA-2P (scale bar, 4 mm) and NTERA-2R (scale bar, 5 mm) tumors. Slides were scanned using an Aperio CS2 scanner (Leica Microsystems, Inc.) at a magnification of x20. (B) Tumor growth curve of NTERA-2P (n=3) and NTERA-2R (n=3). (C) Relative mRNA expression levels of *CDH1*, *CDH2*, *VIM*, *SNAIL* and *SLUG* in NTERA-2P (n=3) and NTERA-2R tumors (n=3). *P≤0.05. *CDH*, cadherin; NTERA-2P, parental NTERA-2; NTERA-2R, cisplatin-resistant NTERA-2; *SLUG*, snail family transcriptional repressor 2; *SNAIL*, snail family transcriptional repressor 1; *VIM*, vimentin.

histological subtype classification of TGCT, and the transcription factor *SLUG* was involved in PFS and chemoresistance. To the best of our knowledge, the present study was the first to evaluate cisplatin-resistant GCT models, focusing specifically on exploring the EMT regulator *SLUG*.

GCTs are heterogeneous tumors, and it is a challenge to study their genetic basis, especially molecular alternatives that may lead to histological classification of GCTs and improvement of chemoresistance. Studies have explored the molecular complexity and heterogeneity of GCTs by examining the gene expression patterns associated with EMT (36-38). The present study showed that SE, embryonal carcinoma and mixed GCT had different expression profiles for the main EMT markers. For example, SE is a highly curable tumor in most cases (39) due to its sensitivity to DNA damaging agents, and in the present study it exhibited downregulation of EMT markers, suggesting a low association with EMT, and consequently with the processes of chemoresistance and metastasis.

The interplay between EMT and cancer has been addressed in a number of reviews (5,40-43). EMT-related proteins have been analyzed in histological malignant ovarian GCT types; VIM and zinc finger E-box-binding homeobox 1 have been revealed to be significantly increased in immature teratomas compared with in yolk sac tumors and dysgerminomas (44). Growth factors and cytokines are the principal inducers of the EMT process, and they activate several signaling pathways that modulate EMT effectors, including the transcription factors SNAIL and SLUG. These regulatory factors suppress E-cadherin by binding proximal to the E-cadherin promoter at the E-box elements. Subsequently, epithelial cells gradually lose their epithelial characteristics and gain mesenchymal cell properties (1,2,36). SLUG is a transcriptional factor that has been evaluated in several types of human cancer (45-48), and has been reported to be associated with decreased E-cadherin expression, high histological grade, metastasis, postoperative recurrence and short-term survival (49,50). In addition, the high expression of SLUG has been shown to be significantly associated with shorter overall survival of patients with cancer (49,51,52). In breast cancer survival rate analysis, 5-year survival was significantly lower for patients with positive SLUG expression, but only in patients harboring E-cadherin-preserved tumors, suggesting that SLUG may be critical to suppress the expression of E-cadherin (52). In lung adenocarcinoma, the upregulation of SLUG has been shown to be significantly related to postoperative relapse and shorter patient survival (51). Moreover, the overall survival analysis of patients with colorectal carcinoma and SLUG-positive expression was revealed to be poorer, and SLUG expression was identified as an independent prognostic factor (49). Furthermore, the immunohistochemical expression of SLUG and SNAIL has been investigated in patients with different stages of renal cell carcinoma; SLUG exhibited a higher incidence of expression in tumors with a sarcomatoid component. In addition, Kaplan-Meier survival curve analysis revealed no discernible disparity in survival rates relative to SLUG expression within the initial 3 years of follow-up. However, beyond this timeframe, patients whose tumors did not exhibit SLUG expression demonstrated significantly prolonged survival

periods (53). Consistent with these observations, the present study was the first to demonstrated that the high expression of *SLUG* may have significant effects on the PFS of patients with TGCT, suggesting that regulation of *SLUG* could be a therapeutic alternative to improve PFS.

After conducting *in silico* analysis, EMT was evaluated in JEG-3 and NTERA-2 GCT cell lines by examining the expression of EMT markers. Compared with in JEG-3 cells, NTERA-2 cells showed increased expression of mesenchymal markers (*CDH2*, *VIM* and *SLUG*) and decreased expression of an epithelial marker (*CDH1)*. This difference may be explained by the distinct origins of the cell lines: NTERA-2 cells come from embryonal carcinoma, whereas JEG-3 cells originate from choriocarcinoma, and they are different in their cellular differentiation and biological behavior. Embryonal carcinoma cells are pluripotent and resemble early embryonic stem cells, which have the potential to differentiate into several cell types (11). By contrast, choriocarcinoma is a more differentiated form of GCT that resembles placental tissue, specifically trophoblast cells (8). Therefore, embryonal carcinoma cells, due to their less differentiated state and higher plasticity, are more prone to undergo EMT than the more differentiated choriocarcinoma cells.

While TGCT has a high survival rate, some patients develop a tumor relapse after the first treatment or have refractory disease (14). Resistance to chemotherapy may be multifactorial, and EMT is one of the biological processes linked to resistance. The present study elucidated the association between EMT and cisplatin resistance using a cisplatin-resistant model, which showed upregulation of *FN1*, *VIM*, *ACTA2*, *COL1A1*, *TGF-β* and *SLUG* genes. In our previous study, a phenotypic characterization of a cisplatin-resistant model was performed and was shown to exhibit a more aggressive phenotype compared with parental cells (23). This was evidenced by a significant increase in cell proliferation, greater clonogenic survival and higher migration rates. The increase in all of these processes may be closely associated with EMT.

Using a cell line model of cisplatin-resistant ovarian cancer, Haslehurst *et al* (54) showed upregulation of VIM, SNAIL and SLUG, and downregulation of E-cadherin in chemoresistant cells. In addition, the knockdown of *SNAIL* and *SLUG* reversed the EMT phenotype and reduced cellular resistance to cisplatin (54). The crosstalk between STAT3 and p53/RAS signaling controls metastasis and cisplatin resistance in ovarian cancer cells through the SLUG/MAPK/PI3K/AKT-mediated regulation of EMT (55). Taken together, these reports suggest that EMT-related markers may serve a critical role in cisplatin resistance in GCT, thus leading to the establishment of biomarkers of drug response and new potential therapeutic approaches to overcome resistance to chemotherapy. Although EMT significantly impacts drug resistance in several types of cancer, the molecular mechanisms involved are poorly understood.

The present study also revealed that a NTERA-2R mouse model exhibited a significant upregulation in *SLUG* expression. Despite several studies addressing the impact of *SLUG* on drug resistance (56-58), none have analyzed this in the context of GCT. SLUG can increase the chemoresistance of various types of cancer, such as malignant mesothelioma and cholangiocarcinoma. In addition, SLUG overexpression has been shown to assist in apoptosis resistance in leukemic progenitors and may be related to imatinib resistance of chronic myelocytic leukemia (59). SLUG-knockdown may also enhance the sensitivity of neuroblastoma cells to imatinib by downregulating Bcl-2 expression (60). These findings suggest a crucial role of SLUG in drug resistance; therefore, targeting EMT-TFs may be proposed as a novel strategy to treat drug resistance (16).

In conclusion, the present study provided information on the relationship between cisplatin resistance and the EMT process in TGCT. The present investigation into the EMT regulator *SLUG* in TGCT is pioneering, revealing its association with histological subtypes, PFS and chemoresistance. The findings revealed the significance of EMT in the context of cisplatin resistance, highlighting *SLUG* as a potential therapeutic target to improve patient outcomes. These insights suggest that targeting EMT-TFs, such as *SLUG*, may be a promising strategy to overcome drug resistance and enhance therapeutic efficacy in TGCT. However, further elucidation of the molecular mechanisms underlying EMT and drug resistance holds promise for developing novel therapeutic interventions for TGCT.

Acknowledgements

Not applicable.

Funding

The present study was supported by the Fundação de Amparo à Pesquisa do Estado de São Paulo, Brasil (grant nos. 2019/07502-8; 2020/13286-3; 2018/13026-1; 2018/18808-8; 2018/15065-4), the Conselho Nacional de Desenvolvimento Científico e Tecnológico, Brazil (grant no. 121336/2019-0), the Public Ministry of Labor Campinas (Research, Prevention, and Education of Occupational Cancer-15ª zone, Campinas, Brazil) and Researcher Support Program from Barretos Cancer Hospital.

Availability of data and materials

The data generated in the present study may be requested from the corresponding author.

Authors' contributions

MTP conceptualized the study. The experiments were performed by IIVC, MNR, LMBT, LPR, LABP, LS, JMSG, ICT, AVHL and SAT. MTP, MNR, MCDC, RMR, LFL and DAM performed data analysis. LFL was responsible for clinical data of patients. IIVC, MNR, RMR, LFL and MTP wrote the original draft. IIVC, MNR, AVHL, DAM, LS, SAT, RMR, LFL and MTP reviewed and edited the manuscript. RMR, LFL and MTP supervised the project. MTP administered the project. MTP and RMR acquired funding. MTP and IIVC confirm the authenticity of all the raw data. All authors have read and approved the final version of the manuscript.

Ethics approval and consent to participate

The study was approved by the IACUC at Barretos Cancer Hospital (approval no. 010/2020).

Patient consent for publication

Not applicable.

Competing interests

The authors declare that they have no competing interests.

References

1. Kalluri R and Weinberg R: The basics of epithelial-mesenchymal transition. J Clin Invest 119: 1420-1428, 2009.
2. Thiery JP, Acloque H, Huang RYJ and Nieto MA: Epithelial-mesenchymal transitions in development and disease. Cell 139: 871-890, 2009.
3. Yang J and Weinberg RA: Epithelial-mesenchymal transition: At the crossroads of development and tumor metastasis. Dev Cell 14: 818-829, 2008.
4. Ye X and Weinberg RA: Epithelial-mesenchymal plasticity: A central regulator of cancer progression. Trends Cell Biol 25: 675-686, 2015.
5. Kaufhold S and Bonavida B: Central role of Snail1 in the regulation of EMT and resistance in cancer: A target for therapeutic intervention. J Exp Clin Cancer Res 33: 62, 2014.
6. Grasset EM, Dunworth M, Sharma G, Loth M, Tandurella J, Cimino-Mathews A, Gentz M, Bracht S, Haynes M, Fertig EJ and Ewald AJ: Triple-negative breast cancer metastasis involves complex epithelial-mesenchymal transition dynamics and requires vimentin. Sci Transl Med 14: eabn7571, 2022.
7. Tsoukalas N, Aravantinou-Fatorou E, Tolia M, Giaginis C, Galanopoulos M, Kiakou M, Kostakis ID, Dana E, Vamvakaris I, Korogiannos A, *et al*: Epithelial-mesenchymal transition in non small-cell lung cancer. Anticancer Res 37: 1773-1778, 2017.
8. Palamaris K, Felekouras E and Sakellariou S: Epithelial to mesenchymal transition: Key regulator of pancreatic ductal adenocarcinoma progression and chemoresistance. Cancers (Basel) 13: 5532, 2021.
9. Sessa C, Schneider DT, Planchamp F, Baust K, Braicu EI, Concin N, Godzinski J, McCluggage WG, Orbach D, Pautier P, *et al*: ESGO-SIOPE guidelines for the management of adolescents and young adults with non-epithelial ovarian cancers. Lancet Oncol 21: e360-e368, 2020.
10. Ghazarian AA, Kelly SP, Altekruse SF, Rosenberg PS and McGlynn KA: Future of testicular germ cell tumor incidence in the United States: Forecast through 2026. Cancer 123: 2320-2328, 2017.
11. Pierce JL, Frazier AL and Amatruda JF: Pediatric germ cell tumors: A developmental perspective. Adv Urol 2018: 9059382, 2018.
12. Culine S, Kramar A, Théodore C, Geoffrois L, Chevreau C, Biron P, Nguyen BB, Héron JF, Kerbrat P, Caty A, *et al*: Randomized trial comparing bleomycin/etoposide/cisplatin with alternating cisplatin/cyclophosphamide/doxorubicin and vinblastine/bleomycin regimens of chemotherapy for patients with intermediate- and poor-risk metastatic nonseminomatous germ cell tumors: Genito-Urinary Group Of The French Federation Of Cancer Centers Trial T93MP. J Clin Oncol 26: 421-427, 2008.
13. Pinto MT, Cárcano FM, Vieira AGS, Cabral ERM and Lopes LF: Molecular biology of pediatric and adult male germ cell tumors. Cancers (Basel) 13: 2349, 2021.
14. de Vries G, Rosas-Plaza X, van Vugt MATM, Gietema JA and de Jong S: Testicular cancer: Determinants of cisplatin sensitivity and novel therapeutic opportunities. Cancer Treat Rev 88: 102054, 2020.
15. Vega S, Morales AV, Ocaña OH, Valdés F, Fabregat I and Nieto MA: Snail blocks the cell cycle and confers resistance to cell death. Genes Dev 18: 1131-1143, 2004.
16. Saxena M, Stephens MA, Pathak H and Rangarajan A: Transcription factors that mediate epithelial-mesenchymal transition lead to multidrug resistance by upregulating ABC transporters. Cell Death Dis 2: e179, 2011.
17. Wu K and Bonavida B: The activated NF-κB-Snail-RKIP circuitry in cancer regulates both the metastatic cascade and resistance to apoptosis by cytotoxic drugs. Crit Rev Immunol 29: 241-254, 2009.
18. Lee HH, Lee SH, Song KY, Na SJ, O JH, Park JM, Jung ES, Choi MG and Park CH: Evaluation of Slug expression is useful for predicting lymph node metastasis and survival in patients with gastric cancer. BMC Cancer 17: 670, 2017.
19. Gu A, Jie Y, Yao Q, Zhang Y and Mingyan E: Slug is associated with tumor metastasis and angiogenesis in ovarian cancer. Reprod Sci 24: 291-299, 2017.
20. Bhat-Nakshatri P, Appaiah H, Ballas C, Pick-Franke P, Goulet R Jr, Badve S, Srour EF and Nakshatri H: SLUG/SNAI2 and tumor necrosis factor generate breast cells with CD44+/CD24-phenotype. BMC Cancer 10: 411, 2010.
21. Shen H, Shih J, Hollern DP, Wang L, Bowlby R, Tickoo SK, Thorsson V, Mungall AJ, Newton Y, Hegde AM, *et al*: Integrated molecular characterization of testicular germ cell tumors. Cell Rep 23: 3392-3406, 2018.
22. Gu Z, Eils R and Schlesner M: Complex heatmaps reveal patterns and correlations in multidimensional genomic data. Bioinformatics 32: 2847-2849, 2016.
23. Lengert AVH, Pereira LDNB, Cabral ERM, Gomes INF, Jesus LM, Gonçalves MFS, Rocha AOD, Tassinari TA, Silva LSD, Laus AC, *et al*: Potential new therapeutic approaches for cisplatin-resistant testicular germ cell tumors. Front Biosci (Landmark Ed) 27: 245, 2022.
24. Silva-Oliveira RJ, Silva VAO, Martinho O, Cruvinel-Carloni A, Melendez ME, Rosa MN, de Paula FE, de Souza Viana L, Carvalho AL and Reis RM: Cytotoxicity of allitinib, an irreversible anti-EGFR agent, in a large panel of human cancer-derived cell lines: KRAS mutation status as a predictive biomarker. Cell Oncol (Dordr) 39: 253-263, 2016.
25. Pfaffl MW: A new mathematical model for relative quantification in real-time RT-PCR. Nucleic Acids Res 29: e45, 2001.
26. Teixeira SA, Luzzi MC, Martin ACBM, Duarte TT, Leal MO, Teixeira GR, Reis MT, Junior CRA, Santos K, Melendez ME, *et al*: The barretos cancer hospital animal facility: Implementation and results of a dedicated platform for preclinical oncology models. Vet Sci 9: 636, 2022.
27. Mikami S, Katsube KI, Oya M, Ishida M, Kosaka T, Mizuno R, Mukai M and Okada Y: Expression of Snail and Slug in renal cell carcinoma: E-cadherin repressor Snail is associated with cancer invasion and prognosis. Lab Invest 91: 1443-1458, 2011.
28. Gerwing M, Jacobsen C, Dyshlovoy S, Hauschild J, Rohlfing T, Oing C, Venz S, Oldenburg J, Oechsle K, Bokemeyer C, *et al*: Cabazitaxel overcomes cisplatin resistance in germ cell tumour cells. J Cancer Res Clin Oncol 142: 1979-1994, 2016.
29. Wang J, Wei Q, Wang X, Tang S, Liu H, Zhang F, Mohammed MK, Huang J, Guo D, Lu M, *et al*: Transition to resistance: An unexpected role of the EMT in cancer chemoresistance. Genes Dis 3: 3-6, 2016.
30. Smith B and Bhowmick N: Role of EMT in metastasis and therapy resistance. J Clin Med 5: 17, 2016.
31. Tang LH, Gonen M, Hedvat C, Modlin IM and Klimstra DS: Objective quantification of the Ki67 proliferative index in neuroendocrine tumors of the gastroenteropancreatic system: A comparison of digital image analysis with manual methods. Am J Surg Pathol 36: 1761-1770, 2012.
32. Klimowicz AC, Bose P, Petrillo SK, Magliocco AM, Dort JC and Brockton NT: The prognostic impact of a combined carbonic anhydrase IX and Ki67 signature in oral squamous cell carcinoma. Br J Cancer 109: 1859-1866, 2013.
33. Fukawa T and Kanayama H: Current knowledge of risk factors for testicular germ cell tumors. Int J Urol 25: 337-344, 2018.
34. Rocha CRR, Silva MM, Quinet A, Cabral-Neto JB and Menck CFM: DNA repair pathways and cisplatin resistance: An intimate relationship. Clinics (Sao Paulo) 73 (Suppl 1): e478s, 2018.
35. Brasseur K, Gévry N and Asselin E: Chemoresistance and targeted therapies in ovarian and endometrial cancers. Oncotarget 8: 4008-4042, 2017.
36. Antony J, Thiery JP and Huang RYJ: Epithelial-to-mesenchymal transition: Lessons from development, insights into cancer and the potential of EMT-subtype based therapeutic intervention. Phys Biol 16: 041004, 2019.
37. Wakileh GA, Bierholz P, Kotthoff M, Skowron MA, Bremmer F, Stephan A, Anbuhl SM, Heukers R, Smit MJ, Ströbel P and Nettersheim D: Molecular characterization of the CXCR4/CXCR7 axis in germ cell tumors and its targetability using nanobody-drug-conjugates. Exp Hematol Oncol 12: 96, 2023.

38. Bremmer F, Schallenberg S, Jarry H, Küffer S, Kaulfuss S, Burfeind P, Strauß A, Thelen P, Radzun HJ, Ströbel P, *et al*: Role of N-cadherin in proliferation, migration, and invasion of germ cell tumours. Oncotarget 6: 33426-33437, 2015.
39. Classen J, Souchon R, Hehr T and Bamberg M: Treatment of early stage testicular seminoma. J Cancer Res Clin Oncol 127: 475-481, 2001.
40. De Las Rivas J, Brozovic A, Izraely S, Casas-Pais A, Witz IP and Figueroa A: Cancer drug resistance induced by EMT: Novel therapeutic strategies. Arch Toxicol 95: 2279-2297, 2021.
41. Lu W and Kang Y: Epithelial-mesenchymal plasticity in cancer progression and metastasis. Dev Cell 49: 361-374, 2019.
42. Singh A and Settleman J: EMT, Cancer stem cells and drug resistance: An emerging axis of evil in the war on cancer. Oncogene 29: 4741-4751, 2010.
43. Singh D and Siddique HR: Epithelial-to-mesenchymal transition in cancer progression: Unraveling the immunosuppressive module driving therapy resistance. Cancer Metastasis Rev 43: 155-173, 2024.
44. Solheim O, Førsund M, Tropé CG, Kraggerud SM, Nesland JM and Davidson B: Epithelial-mesenchymal transition markers in malignant ovarian germ cell tumors. APMIS 125: 781-786, 2017.
45. Schinke H, Pan M, Akyol M, Zhou J, Shi E, Kranz G, Libl D, Quadt T, Simon F, Canis M, *et al*: SLUG-related partial epithelial-to-mesenchymal transition is a transcriptomic prognosticator of head and neck cancer survival. Mol Oncol 16: 347-367, 2022.
46. Kim H, Lee SB, Myung JK, Park JH, Park E, Il Kim D, Lee C, Kim Y, Park CM, Kim MB, *et al*: SLUG is a key regulator of Epithelial-Mesenchymal transition in pleomorphic adenoma. Lab Invest 102: 631-640, 2022.
47. Noguchi S, Hirano K, Tanimoto N, Shimada T and Akiyoshi H: SLUG is upregulated and induces epithelial mesenchymal transition in canine oral squamous cell carcinoma. Vet Comp Oncol 20: 134-141, 2022.
48. Önder E, Çil N, Seçme M and Mete GA: Effect of alpha lipoic acid on epithelial mesenchymal transition in SKOV-3 cells. Gene 892: 147880, 2024.
49. Alves CC, Carneiro F, Hoefler H and Becker KF: Role of the epithelial-mesenchymal transition regulator Slug in primary human cancers. Front Biosci (Landmark Ed) 14: 3035-3050, 2009.
50. Shih JY and Yang PC: The EMT regulator slug and lung carcinogenesis. Carcinogenesis 32: 1299-1304, 2011.
51. Shih JY, Tsai MF, Chang TH, Chang YL, Yuan A, Yu CJ, Lin SB, Liou GY, Lee ML, Chen JJ, *et al*: Transcription repressor slug promotes carcinoma invasion and predicts outcome of patients with lung adenocarcinoma. Clin Cancer Res 11: 8070-8078, 2005.
52. Martin TA, Goyal A, Watkins G and Jiang WG: Expression of the transcription factors snail, slug, and twist and their clinical significance in human breast cancer. Ann Surg Oncol 12: 488-496, 2005.
53. Zivotic M, Kovacevic S, Nikolic G, Mioljevic A, Filipovic I, Djordjevic M, Jovicic V, Topalovic N, Ilic K, Radojevic Skodric S, *et al*: SLUG and SNAIL as potential immunohistochemical biomarkers for renal cancer staging and survival. Int J Mol Sci 24: 12245, 2023.
54. Haslehurst AM, Koti M, Dharsee M, Nuin P, Evans K, Geraci J, Childs T, Chen J, Li J, Weberpals J, *et al*: EMT transcription factors snail and slug directly contribute to cisplatin resistance in ovarian cancer. BMC Cancer 12: 91, 2012.
55. Liang F, Ren C, Wang J, Wang S, Yang L, Han X, Chen Y, Tong G and Yang G: The crosstalk between STAT3 and p53/RAS signaling controls cancer cell metastasis and cisplatin resistance via the Slug/MAPK/PI3K/AKT-mediated regulation of EMT and autophagy. Oncogenesis 8: 59, 2019.
56. Oh SJ, Ahn EJ, Kim O, Kim D, Jung TY, Jung S, Lee JH, Kim KK, Kim H, Kim EH, *et al*: The role played by SLUG, an Epithelial-Mesenchymal transition factor, in invasion and therapeutic resistance of malignant glioma. Cell Mol Neurobiol 39: 769-782, 2019.
57. Shen CJ, Kuo YL, Chen CC, Chen MJ and Cheng YM: MMP1 expression is activated by Slug and enhances multi-drug resistance (MDR) in breast cancer. PLoS One 12: e0174487, 2017.
58. Chang L, Hu Y, Fu Y, Zhou T, You J, Du J, Zheng L, Cao J, Ying M, Dai X, *et al*: Targeting slug-mediated non-canonical activation of c-Met to overcome chemo-resistance in metastatic ovarian cancer cells. Acta Pharm Sin B 9: 484-495, 2019.
59. Mancini M, Petta S, Iacobucci I, Salvestrini V, Barbieri E and Santucci MA: Zinc-finger transcription factor slug contributes to the survival advantage of chronic myeloid leukemia cells. Cell Signal 22: 1247-1253, 2010.
60. Vitali R, Mancini C, Cesi V, Tanno B, Mancuso M, Bossi G, Zhang Y, Martinez RV, Calabretta B, Dominici C and Raschellà G: Slug (SNAI2) Down-Regulation by RNA interference facilitates apoptosis and inhibits invasive growth in neuroblastoma preclinical models. Clin Cancer Res 14: 4622-4630, 2008.